Flexible Gel Polymer Electrolytes Based on Carboxymethyl Cellulose Blended with Polyvinyl Alcohol or Polyacrylic Acid for Zinc-Air Batteries

Estibaliz García-Gaitán,[a, b, c] Domenico Frattini,[a] Idoia Ruiz de Larramendi,[b]
María Martínez-Ibáñez,[a] Daniel González,[c] Michel Armand,[a] and
Nagore Ortiz-Vitoriano*[a, d]

Flexible zinc-air batteries are based on gel polymer electrolytes (GPE), soft, semi-solid components devoted to liquid electrolyte retention, ion conduction, and mechanical stability. Many synthetic polymers, and their blends, have been used in early works due to the good compromise between ionic conductivity, electrolyte retention, and mechanical resistance. Naturally occurring biopolymers are a great alternative to increase the sustainability of GPE, but present properties are not sufficient. In this work, the blending of carboxymethyl cellulose (CMC) with polyvinyl alcohol (PVA) or polyacrylic acid (PAA) is studied together with synthesis, cross-linking, and liquid electrolyte embedding method. The CMC:PAA (1:2) composite, with ex-situ gel embedding of 8 M KOH electrolyte achieved ionic conductivity of 0.231 S cm^{-1} at room temperature, high liquid electrolyte uptake and retention, providing a 78% of zinc utilization and 443.19 Wh kg^{-1} as energy density for assembled primary zinc-air battery. The CMC:PAA and CMC:PVA also showed unexpected self-healing behavior activated by re-wetting with liquid KOH solution and drying.

Introduction

Flexible gel polymer electrolytes (GPEs) represent the core component of advanced power sources for smart and wearable devices,[1] where zinc-air batteries (ZABs) are particularly promising thanks to the high specific energy density, low cost, abundant raw materials, intrinsic safety, and the possibility to directly use environmental air to produce electricity.[2,3] However, when operating these flexible batteries, major issues arise from evaporation and leakage of the electrolyte, as well as possible mechanical damages due to irreversible breaks in the GPE, hence a high liquid electrolyte uptake/retention combined with sufficient flexibility and mechanical resistance would be desired.[4] Nevertheless, the disposal of the device after use should be safe and eco-friendly. Hence, for the design of a GPE,

selection of polymer, formulation, additives, and manufacturing process contribute to the preferred properties.[5] In previous reports, the progress achieved by GPEs in flexible devices was carefully analyzed[6,7] showing that the major focus is on intercalation-based devices, like flexible supercapacitors, lithium-ion and zinc-ion batteries, with small attention to conversion-based devices like ZABs. Some of these GPEs can be also applied in ZABs depending on the liquid electrolyte and materials used, because the polymer matrix has channels for both positive/negative ion migration[8] and, differently from intercalation-based devices, in ZABs the charge carrier is the OH$^-$ anion and not the metal cation (e.g., Li$^+$ or Zn^{2+}). However, regardless of the type of device, GPE synthesis and preparation are fundamental aspects in determining properties, full cell performances, and industrial scalability, especially in ZABs. For example, ionic conductivity is dependent on the method to embed the KOH liquid electrolyte in the GPE and the concentration used. For this purpose, two options are possible: directly embedding, partially or completely, the KOH solution at the desired concentration during GPE synthesis (hereafter indicated as *in-situ*), or embedding later the liquid electrolyte by soaking, simple immersion, etc. of the GPE in the electrolyte solution (hereafter indicated as *ex-situ*). For the *in-situ* embedding, the selected polymer should be soluble in the aqueous solution, at the desired KOH concentration, and the resulting gel must have a very high electrolyte retention capability, so that the GPE contains exactly the proper amount of liquid electrolyte at the optimal concentration; for the *ex-situ* embedding, the prepared GPE should have enough electrolyte uptake (other than high electrolyte retention) and limited swelling, to absorb a reasonable amount of KOH liquid electro-

[a] E. García-Gaitán, Dr. D. Frattini, Dr. M. Martínez-Ibáñez, Prof. M. Armand, Dr. N. Ortiz-Vitoriano
Centre for Cooperative Research on Alternative Energies (CIC energiGUNE), Basque Research and Technology Alliance (BRTA)
Alava Technology Park, Albert Einstein 48, 01510, Vitoria-Gasteiz Spain
E-mail: nortiz@cicenergigune.com

[b] E. García-Gaitán, Dr. I. Ruiz de Larramendi
Department of Organic and Inorganic Chemistry, University of the Basque Country (UPV/EHU), Barrio Sarriena s/n, 48940, Leioa, Spain

[c] E. García-Gaitán, D. González
CEGASA Energía SLU, Marie Curie, 1, Parque Tecnológico de Álava, 01510, Miñano, Spain

[d] Dr. N. Ortiz-Vitoriano
Ikerbasque, Basque Foundation for Science, María Díaz de Haro 3, 48013, Bilbao, Spain

lyte avoiding excessive volume change and the use of highly concentrated KOH solutions. In ZABs, it is well known in the literature[9] that the maximum OH− ionic conductivity of KOH solutions falls between 6–8 M, at room temperature and therefore these are the concentrations considered throughout the present work.

Similarly to intercalation-based devices,[6,7] any GPEs reported in the literature for flexible ZABs are fully based on synthetic polymers, like polyvinyl alcohol (PVA), polyacrylic acid (PAA), polyethylene oxide (PEO), and their blends, that increase the carbon footprint of GPE, although giving high ionic conductivity. Naturally occurring biopolymers are being extensively studied in recent years as a greener alternative in energy storage devices,[10] and in ZABs as well. Carboxymethyl cellulose (CMC) is a well-known and cheap derivate product from cellulose, which is a natural and non-synthetic biopolymer, that can be used to prepare more sustainable gels[11,12] with good uptake/retention properties but, unfortunately, the ionic conductivities reported so far are lower than synthetic-based GPEs.[13] The actual state-of-the-art is jeopardized, and various combinations of GPEs based on CMC, PEO, PVA, PAA, and their blends, can be found, but with scarce attention to the correlation between synthesis, electrolyte uptake, ionic conductivity, and performance. For example, Fu et al.[14] prepared a quaternary ammonium-functionalized nanocellulose (QAFC) GPE and adopted *ex-situ* embedding by soaking the membrane in 1 M KOH. They reported an ionic conductivity of 0.021 S cm⁻¹, 492 mAh g$_{Zn}^{-1}$ full discharge capacity (at 25 mA g⁻¹ current density), and a Zn utilization approx. 60%. The same GPE was used in a follow-up work,[15] giving approx. 79% Zn utilization (at 5 mA cm⁻²), but using different assembly and electrode materials, so the beneficial contribution of the developed GPE should be further assessed. In another work, Zhu et al.[16] reported a PAA-based membrane prepared by *in-situ* embedding of 8.4 M KOH, achieving an ionic conductivity of 0.29 S cm⁻¹, 530 mAh g$_{Zn}^{-1}$ full discharge capacity (at 25 mA cm⁻²) for a 64.6% Zn utilization, while Kwon et al.,[17] by preparing a similar PAA-based gel (using 6 M KOH *in-situ*, 10 wt% in the gel) claim 85% Zn utilization (at 1 mA cm⁻²) in small flexible ZABs (ionic conductivities not reported). In general, cross-comparisons of gels are very difficult because recipes are not standardized; final KOH concentrations and liquid electrolyte amounts are not systematically varied, and cell assembly and electrode materials are different. In an early work,[18] GPEs based on PVA:PAA blends were systematically studied by varying PAA content, but the KOH liquid electrolyte was *ex-situ* embedded (7.4 M KOH), electrolyte uptake data not reported, and a pure PAA reference gel was missing, so correlation between blending, amount of absorbed KOH solution, and cell performance cannot be generalized. GPEs with both natural/synthetic biopolymers have been recently proposed,[19] but not yet systematically applied to ZABs, and could be a smart way to tune physico-chemical properties. If not properly controlled, both *in-situ* and *ex-situ* approaches may deliver GPEs for ZABs with non-optimal KOH concentrations, and the benefits of blending natural and synthetic

biopolymers into a hybrid GPEs, could be underestimated, as well as performance, and more methodical works are needed.

The methodical novelties proposed in this study are: (i) the rational design and blending of GPEs including CMC, PAA, or PVA; (ii) the consolidated use of 6 or 8 M KOH liquid electrolyte to obtain the maximum ionic conductivity; (iii) the consistent comparison of the benefits attributable to the *in-situ* or *ex-situ* gel electrolyte embedding strategy. These novelties aim to determining the best practice for liquid electrolyte embedding, the reduction of KOH concentration for soaking solutions, and the minimal amount of synthetic polymer to obtain the best possible GPE for primary ZABs. In addition, instead of using the freeze-thawing method,[20–23] which is the most popular, in this work, the blended membranes have been prepared by exploring various alternative methods and recipes. The final recipes developed in this work are optimized to obtain easy procedures and reproducible results and are reported in the supporting information. Moreover, the state of the art generally reports the use of more than 5 wt% of polymer for developing GPEs, as for example in,[17,24,25] whereas in this study 3–5 wt% of total mass of solid (polymers) was required, representing a further novelty of the developed approach. Thermal and chemical behavior of the blended GPEs are studied, together with physical KOH solution uptake and ionic conductivity. Finally, full cell performances under "fast" discharge (5 mA cm⁻²) of the various gels are determined and compared to demonstrate the potential application of the developed approach.

Results and Discussion

Physico-chemical characterization of the developed membranes was carried out using a wide range of techniques such as Fourier-transform infrared spectroscopy (FTIR), thermogravimetry analysis (TGA), differential thermal analysis (DTA), gravimetric KOH liquid electrolyte uptake, weight loss and electrochemical impedance spectroscopy (EIS) for ionic conductivity.

The FTIR spectra present a broad band between 3600 and 3100 cm⁻¹, assigned to the stretching vibration modes of −OH groups (Figures 1 and 2).

This region of the spectrum could also be related to both intermolecular and intramolecular hydrogen bonds. The reference FTIR spectrum of the KOH 8 M liquid electrolyte (in orange in Figures 1e and 2e) shows two characteristic peaks. The −OH stretching vibration is observed at 3320 cm⁻¹ and the band related to H−O−H bending vibration of bound/adsorbed water at 1645 cm⁻¹. For CMC (Figures 1a and 2a), a signal centered at 2900 cm⁻¹ relative to the C−H asymmetric stretching vibration can be distinguished. Regarding the symmetric and asymmetric stretching vibrations of the carboxylate groups, the corresponding peaks can be observed at 1411 and 1587 cm⁻¹, respectively. Between 1200 and 900 cm⁻¹ the vibrations are assigned to C−O−C and C−OH stretching within the polysaccharide skeleton. In PVA, characteristic bands can be observed in the FTIR spectrum shown in Figure 1(b). The −CH₂− and
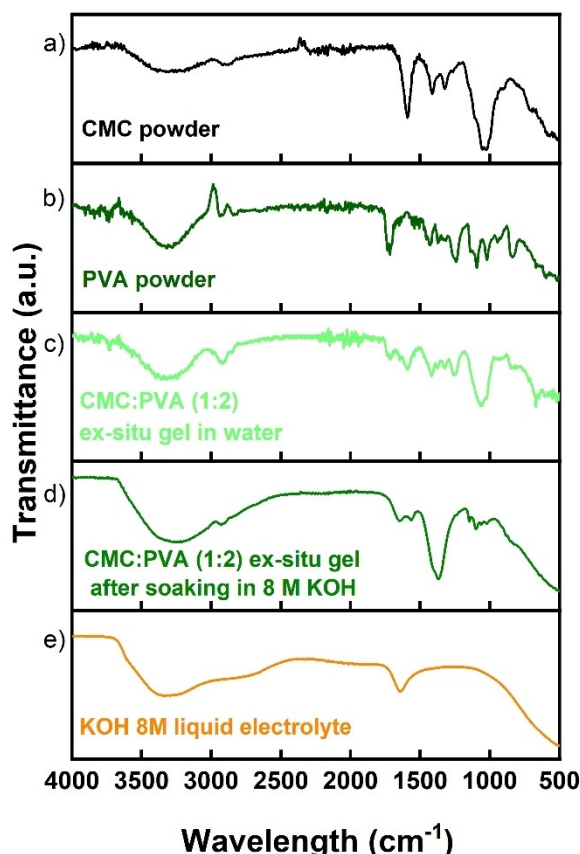
Figure 1. FTIR spectra of a) CMC powder, b) pure PVA, c) CMC:PVA (1:2) *ex-situ* gel prepared in water an d) CMC:PVA (1:2) *ex-situ* gel after soaking in 8 M KOH, e) KOH 8 M liquid electrolyte.
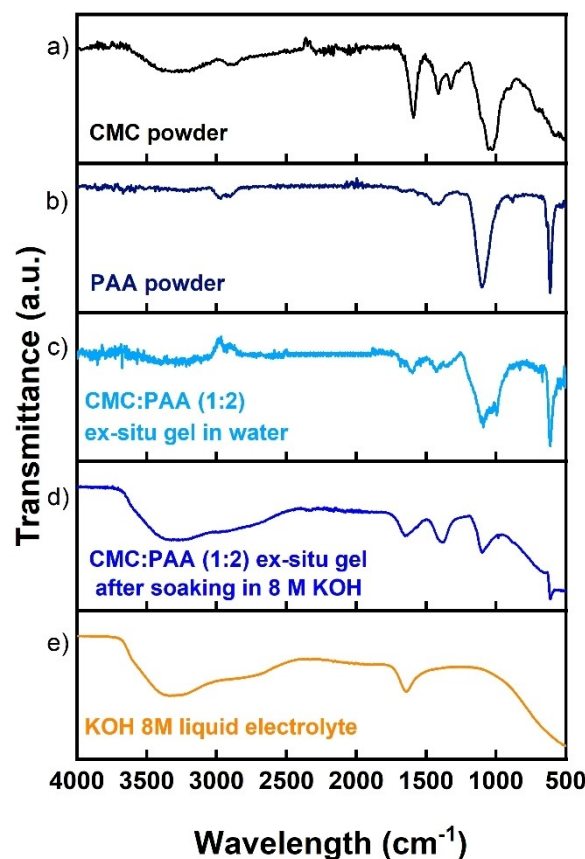

Figure 2. FTIR spectra of a) CMC powder, b) pure PAA, c) CMC:PAA (1:2) *ex-situ* gel prepared in water, d) CMC:PAA (1:2) ex-situ gel after soaking in 8 M KOH, e) KOH 8 M liquid electrolyte.

—CH— stretching vibrations are observable at 2930 and at 2830 cm^{-1}, respectively.[26] Other characteristic signal of the PVA spectrum corresponds to the C—O stretching vibration that appears at 1730 cm^{-1}. Additionally, bands corresponding to the presence of acetate groups remaining from the synthesis of PVA are also distinguishable as the band corresponding to C=O mode (~1720 cm^{-1}).[27] The spectrum corresponding to the *ex-situ* gel of CMC and PVA (without KOH electrolyte, Figure 1c) shows the characteristic bands of the hydroxyl group (3500–3100 cm^{-1}), alkyl group (2970–2850 cm^{-1}) and acetate groups remaining in the PVA structure (1730–1720 cm^{-1} and between 1200 and 900 cm^{-1}), together with those bands of the vibrations of C—O—C and C—OH stretching on polysaccharide skeleton in the CMC. This spectrum is related to a mixture of both components, observing a higher intensity of the bands corresponding to PVA, in good agreement with a CMC:PVA weight ratio of 1:2. On the other hand, when CMC and PVA are mixed and soaked in KOH, the spectrum (Figure 1d) presents small differences. The bands corresponding to the —OH stretching and bending vibrations of KOH liquid electrolyte and PVA, at 3400 and 1375 cm^{-1}, respectively, are clearly distinguished suggesting the rise of strong H bonds between the polymer matrix and the added electrolyte. Furthermore, it is possible to appreciate at 2933 and 2866 cm^{-1} the asymmetric and symmetric stretching vibrations of the —CH$_2$ group,

respectively. At 1088 cm^{-1} the peak corresponding to the C—O stretching vibration is also observed. The band at 1655 cm^{-1} can be associated with vibrational bands of the C=O group, probably due to a physical crosslinking between PVA and CMC in presence of KOH.[28,29] This crosslinking can be helpful in terms of GPE stability. When adding KOH into the membrane formulation, the disappearance of the bands assigned to the vibrations of the acetate groups remaining in the PVA structure implies a potential hydrolysis reaction of the acetyl groups by the presence of the —OH groups.[27] In the case of the CMC:PAA gel (Figure 2d), a similar behavior is observed, although the intensity of the peak at 1360 cm^{-1} due to the O—H bending vibrations of the PAA polymer is less intense than that for PVA. The peak related to the vibration of the C=O group, on the other hand, presents a higher relative intensity in the case of PAA, which is in good agreement with the presence of the —COO— group in the polymer.

The TGA thermograms of the CMC and PVA powders and the CMC:PVA gel in Figure 3(a) show the difference in weight loss trends while increasing the temperature. It seems that *ex-situ* GPEs are thermally more stable after absorbing the 8 M KOH solution. They retain the liquid electrolyte up to 222 °C with a mass loss of 44.03 % and only lose 60.41 % of the total mass up to 500 °C. On the contrary, the CMC:PVA (1:2) gel prepared in water (i.e., before soaking) shows a total weight
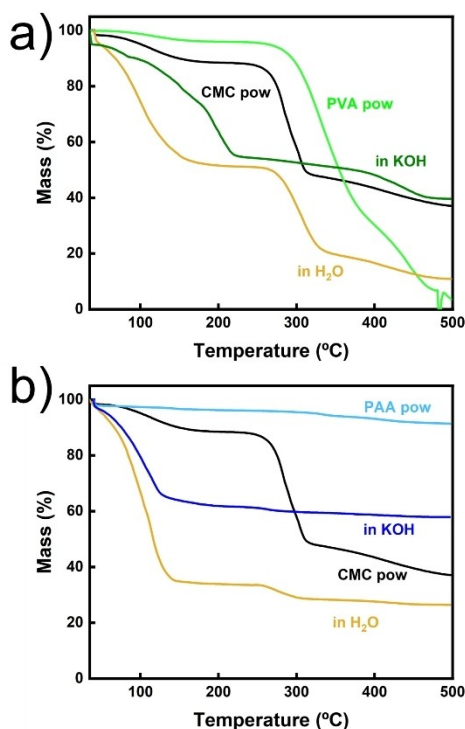
Figure 3. Thermograms of CMC:biopolymer *ex-situ* gels: a) TGA of CMC and PVA powders are shown as well as the CMC:PVA (1:2) *ex-situ* gel prepared in water (bright gold) and CMC:PVA (1:2) *ex-situ* gel after soaking in 8 M KOH (dark green); b) TGA of CMC and PAA powders are shown as well as the CMC:PAA (1:2) *ex-situ* gel prepared in water (bright gold) and CMC:PAA (1:2) *ex-situ* gel after soaking in 8 M KOH (dark blue).

Figure 4. Liquid KOH electrolyte uptake in mass percentage during the *ex-situ* soaking process.

loss of 88.11% up to 500°C. Hence, the gel immersed in an 8 M KOH solution seems more thermally stable. Figure 3(b) shows a similar behavior with the CMC:PAA (1:2) gel. If the membrane is immersed in an 8 M KOH solution, only 42.1% of total mass is lost up to 500°C, whereas if it is not immersed, this results in a 73.55% total mass loss. Once again, the *ex-situ* soaking in KOH helps to prevent mass loss and enhances the thermal stability of the gels. However, it is remarkable that polyacrylic acid precursor is thermally very stable; there is almost no mass loss during the thermogram. It is reported that linear polyacrylic acid polymer has three-stage degradation: 1) formation of anhydride ring between carboxylic acid groups, while water is released, 2) decarboxylation by opening of the anhydride ring, releasing CO_2, and 3) thermal degradation of backbone.[30,31] However, according to Price et al.,[31] the stability of the PAA can be enhanced if it is salified with salts like Na and Ca salts. This can be applied to our case due to the partial potassium salt-form of the used precursor for PAA.

The KOH liquid electrolyte solution uptake of the CMC-based membranes designed herein can be seen in Figure 4. It exceeds values of 100%, being higher in the case of PAA. This effect in the CMC:PAA composite is related to the different chemical crosslinking and the interactions between water and free volume of the biopolymer matrix, as observed in FTIR and TGA-DTA data of the two different polymer blends. Furthermore, the presence of carboxylic groups in the chemical
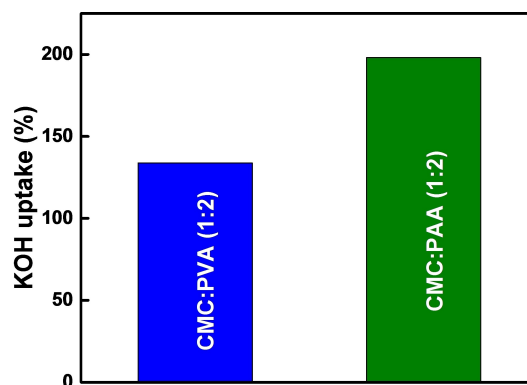
structure of PAA favors intermolecular interactions with the liquid electrolyte through the establishment of hydrogen bonds. These interactions facilitate greater stability of the aqueous KOH solution in the PAA environment. The KOH uptake is an important index directly related to swelling behavior and ionic conductivity.[32] The alkaline CMC-based electrolytes transport the OH⁻ ions acting as anionic exchange membranes. This transport of the hydroxyl anions depends on the amount of water and the KOH concentration within the polymer structure.[33] The conduction of OH⁻ ions in the electrolyte is mainly governed by the Grotthuss mechanism, although diffusion or migration processes must also be considered.[27,34] In this sense, the presence of the aqueous KOH solution in the membrane causes a weakening of the interactions between the polymer chains, which will phase-separate, providing a better pathway with wider channels for the conduction of OH⁻ ions. Thus, the amount of KOH that is embedded in the membrane plays a critical role in order to increase the ionic conductivity.

Physical crosslinking between polymer chains is another factor that can affect the amount of KOH solution that is able to permeate the gel.[35] Higher crosslinking in the polymer prevents the separation between the chains, giving rise to narrower channels, thus hindering the ingress of KOH and consequently the movement of anions through the gel.[5] Acetate groups that have not initially reacted in the PVA synthesis lead to higher crosslinking in the polymer, which hinders KOH adsorption within the CMC:PVA composite. Secondly, although PVA and PAA are both hygroscopic, PVA tends to precipitate in concentrated KOH solutions (>3 M), hence the lower uptake of the CMC:PVA could be also ascribed to the earlier saturation of this gel due to the highly concentrated (8 M) KOH solution used for soaking.

One of the reasons to replace liquid electrolytes and separators in ZABs is because of the low stability and durability they offer once exposed to air. Liquid electrolytes in technologies open to air, such as ZABs, tend to evaporate causing a decrease in ionic conductivity during operation,[25] consequently, it is important to analyse electrolyte retention over time. To quantify this aspect, CMC:biopolymer (1:2) *ex-situ* gels have been tested for liquid electrolyte retention for 50 h.

CMC:PAA gel only loses 4.08%, whereas CMC:PVA membranes 17.79%, after this period of time. In a similar test, PAA gels, with/without additives, showed a far larger electrolyte uptake ($\gg$100%), but also weight losses between 40%–45% after 48 h,[25] confirming that if the liquid electrolyte is added in excessive amounts to compensate evaporation, could cause a leakage instead of retarding evaporation, this is why it is important to improve uptake, but also electrolyte retention. Therefore, a greater liquid electrolyte retention capacity of CMC:PAA membrane is observed compared to those of CMC:PVA, and pure PAA gels from the literature, possibly due to the effect of blending and crosslinking with CMC, supporting the KOH uptake data.

Although initially not a target within this study, the membranes were found to exhibit interesting self-healing behavior. This phenomenon is visually depicted in Figure 5. CMC-based membranes combined with PVA or PAA were shaped after being immersed in 8 M KOH solution. These membranes were deliberately chopped and, subsequently, the obtained pieces were fixed together by adding an 8 M KOH aqueous solution. As can be seen in Figure 5(a), the pieces healed back together. These new self-healing membranes can be dried at 60 °C for several hours.

Before reaching complete dryness, they are removed from the oven. These membranes have adequate mechanical properties to be able to be machined again, being possible to cut them at the necessary dimensions to integrate them back into the battery. Figure 5(b) shows the healing of a CMC:PAA membrane that has been cut. When wetting it with the 8 M KOH aqueous solution, the integrity of the membrane is restored. A major drawback from which batteries suffer is associated with irreversible changes that occur in the system during operation. These changes are most critical during the cycling of secondary batteries, but primary batteries also suffer from a loss in performance due to these processes.[2] Such changes can be caused by a variety of phenomena, including degradation of functional components (e.g., anode, cathode, current collectors, electrolyte, separator) and the interfaces between such components.[36] The electrolyte within the battery is exposed to compressive forces that can cause cracks and fissures to appear, leading to failure of device performance. This type of degradation is especially critical in the case of

flexible devices that use a solid electrolyte.[37] The membranes analyzed in this study present an intrinsic self-healing behavior due to the formation of reversible bonds. A fracture in the membrane produces the rupture of interactions between the chains. By re-wetting the membrane, these interactions between polymer chains are restored. Interactions between PVA or PAA chains are due to the formation of hydrogen bonds, which are dipole-dipole directional attractive forces. For H bond formation, the presence of a high electronegative small atom (−O) is necessary that can interact with an H atom bonded to another small and highly electronegative atom (−OH group). This reversible self-repair is based, then, on the formation of non-covalent bonds between the polymer chains capable of healing the mechanical damage. The two parts recombine and thus close the fissures which lead to healing. Several authors have recognized that the next generation of energy storage systems will be focused on the development of smart devices that are capable of self-repair.[34,38,39] These CMC-based membranes with PVA or PAA constitute a new generation of self-healable electrolytes for ZABs, achieving their self-repair after being cut and revealing a rapid and intrinsic self-restoring capability.

The ionic conductivity of developed membrane was measured and compared to liquid electrolytes,[9] and pure CMC membrane. The results are shown in Figure 6. In Figure 6(a), the two reference KOH liquid electrolytes represent the highest conductivity values at room temperature (0.627 S cm^{-1} 6 M KOH, and 0.598 S cm^{-1} 8 M KOH).[9]

The gel membranes, although being composed of 95% by weight of liquid and the rest being the biopolymer, present lower conductivity, especially the pure CMC in 6 M KOH (with 0.156 S cm^{-1}), and 5 wt% CMC in 8 M KOH (with 0.22 S cm^{-1}), and the copolymer CMC:PVA 1:2 *ex-situ* (0.054 S cm^{-1}). However, the CMC membranes prepared by *in-situ* embedding shows an ionic conductivity three-four times higher (Figure 6a) than CMC:PVA, prepared by *ex-situ* embedding. The CMC:PAA *ex-situ* has a slightly higher ionic conductivity (0.231 S cm^{-1}), being the highest among the studied membranes. This can be ascribed to the superior KOH uptake and water retention of the CMC:PAA as discussed above. The pure CMC membrane is prone to leakage, and to liquefy, whereas the prepared blends have shown longer retention, suggesting that the *ex-situ*

Figure 5. Optical evidence of self-healing behaviors of a) CMC:PVA (1:2) *ex-situ* 8 M KOH and b) CMC:PAA (1:2) *ex-situ* 8 M KOH.
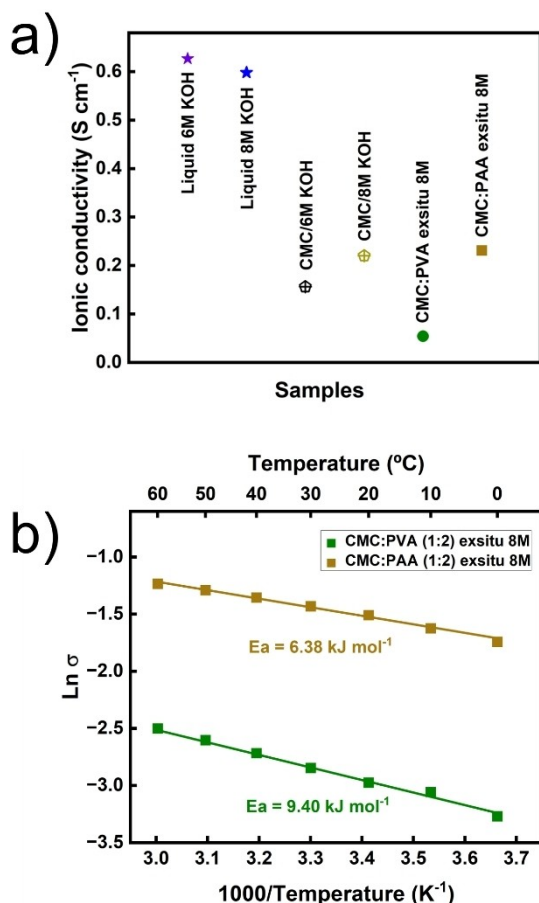
Figure 6. a) Ionic conductivity of membranes and liquid electrolytes at room temperature; b) Arrhenius plot and E_a for *ex-situ* CMC:biopolymer (1:2) membranes.

membranes, the liquid electrolyte has been absorbed by the polymer matrix, thus the evaporation process would be delayed permitting larger migration of ions through the polymer matrix without causing electrolyte loss. The increase in temperature affects the interactions that are established between the polymer chains, weakening them, which translates into a greater spacing between chains and a greater free volume. In this way, the transport of ions through the membrane is more straightforward, thus increasing the ionic conductivity.[40] Activation energy (E_a) is calculated from the Arrhenius plot in Figure 6(b).[41] The two CMC blends have, not only different conductivity, but also different activation energy for ion transport. The E_a is 9.40 kJ mol^{-1} for CMC:PVA (1:2) *ex-situ* and 6.38 kJ mol^{-1} for CMC:PAA (1:2) *ex-situ*. In comparison to literature, both CMC:PVA (1:2) *ex-situ* and CMC:PAA (1:2) *ex-situ* GPEs present lower E_a and higher ionic conductivity. Comparing ionic conductivity and E_a with the literature, for example, employing PVA-KOH based electrolytes, an ionic conductivity of $\approx 10^{-3}$ S cm^{-1} at room temperature, and E_a in the range of 28 and 22 kJ mol^{-1} are reported,[33] whereas in another work[42] ionic conductivity was 0.75×10^{-3} S cm^{-1} and E_a of 0.14 eV (approx. 14–13.5 kJ mol^{-1}). Yang et al.[43,44] disclosed E_a in the range of 3–15 kJ mol^{-1}, which seem to be very low activation energy, however, their PVA-KOH gel electrolytes showed an ionic conductivity ranging between 47–61×10^{-3} S cm^{-1}. The CMC:PVA (1:2) *ex-situ* developed in this work, although worse than CMC:PAA (1:2) *ex-situ*, shows better ionic conductivity and lower E_a than cited references. For PAA-based gels, Zhu et al.[16] prepared a PAA-KOH 6 M gel, reporting 0.288 S cm^{-1} and ≈ 10 kJ mol^{-1} as ionic conductivity and E_a, respectively, very close to the present work, while in another work[25] a similar PAA-KOH 6 M gel achieved 0.127–0.186 S cm^{-1}, lower than the CMC:PAA (1:2) ex-situ developed in this work. Therefore, the E_a achieved are lower than those in other recent works[45,46] and the partial substitution of PAA/PVA with CMC to increase the sustainability seems to not remarkably affect conductivity and E_a. In primary ZABs another important parameter to take into consideration is the capacity of zinc extraction. Galvanostatic discharges were conducted at 5 mA cm^{-2}. Figure 7(a) shows the discharge profiles of CMC membranes varying the concentration of the liquid electrolyte embedded in the polymer matrix. Remarkably, for this CMC-

method is more convenient. In Figure 6(b), the ionic conductivity between 0 °C and 60 °C, which represents a large temperature range to operate a commercial battery, are shown as Arrhenius plot. Numerical values of the conductivity are reported in Table S1. An increase in the temperature drives higher ionic conductivity ought to superior mobility of ions in the GPE. However, increasing the temperature leads also to evaporation, especially in a device open to the air. In these
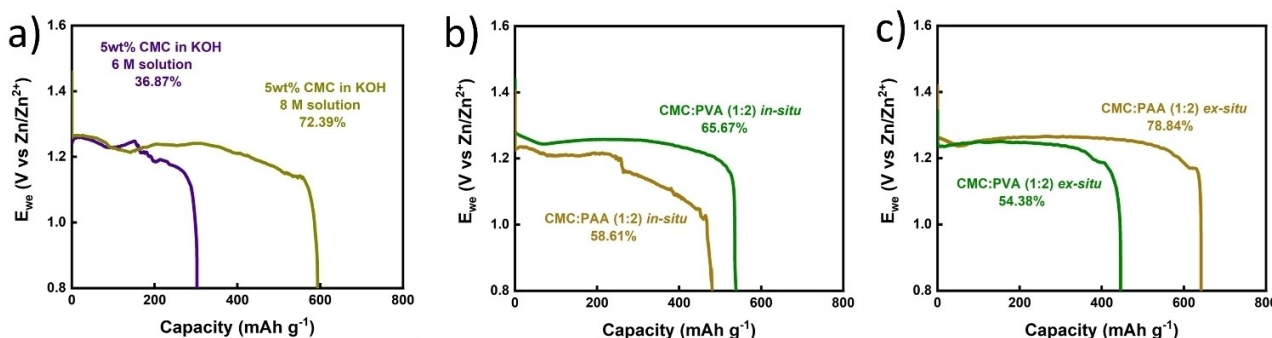

Figure 7. Discharge of primary ZABs: a) pure CMC membranes; b) CMC:PVA (1:2) and CMC:PAA (1:2), *in-situ*; c) CMC:PVA (1:2) and CMC:PAA (1:2) *ex-situ*.

Batteries & Supercaps

Research Article
doi.org/10.1002/batt.202200570

Chemistry Europe
European Chemical
Societies Publishing

based gel, by using 8 M KOH, the discharge capacity, hence Zn extraction, was doubled in comparison to 6 M KOH (72.39% vs. 36.87%). This is why 8 M KOH was used for *ex-situ* gels. However, despite the 72.39% of Zn extraction achieved by the CMC 5 wt% gel, a not negligible liquefaction was detected, as shown in the post-mortem analysis (Figure S1), hence its application is not suitable for ZABs. The blending of biodegradable synthetic polymers (i.e., PAA and PVA) to the CMC matrix resolved this issue when the *ex-situ* electrolyte embedding strategy was used (see Figures S4 and S5) for both PAA and PVA, while *in-situ* embedding did not work for CMC:PVA (1:2) gel (see Figure S2). Concentrated KOH solutions (6-8 M) prevent the formation of the CMC:PVA *in-situ* membranes due to precipitation of the PVA. Even the used dilution of KOH down to 2.7 M did not resolved liquefaction. PAA is soluble and stable in the concentrated KOH solution used, does not precipitate, so CMC:PAA (1:2) *in-situ* membranes were successfully obtained (see Figure S3) and tested. The full discharge of the two *in-situ* CMC:PVA and CMC:PAA gels is reported in Figure 7(b). Only 58.61% of Zn extraction was achieved for the CMC:PAA (1:2) *in-situ*, the profile was noisy, not flat,and not reproducible, whereas the CMC:PVA (1:2) *in-situ* (with 2.7 M KOH), although liquefying, showed a higher Zn extraction of approx. 66%, and a more stable flat profile. To improve the profile of the CMC:PAA (1:2) *in-situ*, the membrane was pressed instead of being punched, achieving a higher Zn extraction (approx. 86%, see Figure S7), but profile was still not flat and discharge voltage lower, and liquefaction was observed. To overcome these issues, the *ex-situ* gels were tested for comparison (Figure 7c). Among them, the CMC:PAA (1:2) *ex-situ* gel presented the highest capacity and Zn extraction, being almost 79% as shown in Figure 7(c). On the contrary, the CMC:PVA (1:2) *ex-situ* gel only achieved approx. 54% of Zn utilization, lower than the CMC:PAA and even lower than its homologous *in-situ*, that achieved approx. 66% (Figure 7b). Reproducible tests are shown in Figures S12–S15 for all the GPEs discussed above. The CMC:PVA did not result in the best mixture because of its poor ionic conductivity (in comparison to the CMC:PAA, see Figure 6a) and its lower discharge capacity, but seems to benefit from the *in-situ* liquid electrolyte embedding approach, whereas the CMC:PAA is best for *ex-situ* embedding. This is an important methodical result to help selection and scaled-up fabrication of GPEs for ZABs that is systematically investigated and clarified in this work. Secondly, the conservation of the flexible property of the developed gels was qualitatively tested by doing a complete folding (i.e., 180° bending) on the membrane (see Figures S8–S10).

The values of specific capacity, Zn extraction, and gravimetric energy density of the cells reported in Figures 7 and S7 are listed in Table S2. For comparison with the literature (not considering the specific cathodes used), Li et al.[24] achieved 550 mAhg_{Zn}^{-1} and 67% Zn extraction in a ZAB assembled with a PVA/KOH (final KOH concentration approx. 0.15 M) *in-situ* gel, very close to the developed CMC:PVA (1:2) *in-situ* gel, but the current density was 3 Acm^{-3}; in another work[47] a similar PVA/KOH *in-situ* gel (1 mL of 18 M KOH was used, final KOH concentration in the gel not reported) achieved 595 mAhg_{Zn}^{-1}

and 73% Zn extraction at a slow discharge current density of 2 mAcm^{-2}, instead of our CMC:PVA (1:2) *in-situ* with 66% Zn extraction but under fast discharge at 5 mAcm^{-2}. For PAA, Kwon et al.[17] used a PAA *in-situ* 6 M KOH gel achieving a very high 684 mAhg_{Zn}^{-1} ($\approx$84% Zn extraction) at 5 mAcm^{-2} (but a very precious Pt–Ir catalyst was used), while Song et al.[25] used a similar PAA *ex-situ* gel soaked in 6 M KOH (and 0.2 M of Zn acetate) in a cell discharged at 2 mAcm^{-2} achieving approx. 40%–60% Zn extraction (values estimated, exact values not reported). The Zn extraction achieved by the CMC:PAA (1:2) *ex-situ* gel are perfectly in line with these examples, and balance the partial substitution of PAA with CMC. Moreover, large gravimetric energy densities were achieved (see Table S2) when the cell is assembled with CMC:PAA (1:2) *ex-situ* gel, providing 443.19 Whkg_{cell}^{-1}, whereas if it is assembled with CMC:PVA (1:2) *ex-situ* gel, the energy density obtained is 294.21 Whkg_{cell}^{-1}. This was possible also thanks to the slightly higher discharge voltage achieved at 5 mAcm^{-2} due to lower overpotentials and higher ionic conductivity. Arai et al.[48] reported that commercial primary ZABs could offer practical energy densities between 250 and 500 Whkg_{cell}^{-1}, depending on the design and weight of the optimized components, so we further support the encouraging energy density achieved in this work with the lab-scale battery assembled with CMC:PAA (1:2) *ex-situ* gel. Therefore, a future optimization and commercialization of a primary ZAB employing a CMC:PAA (1:2) *ex-situ* gel is worthy of further investigation and scale-up, to be used for "fast" discharge up to 5 mAcm^{-2} as current density.

Conclusion

CMC-KOH membranes in the cell environment presented liquefaction issues; therefore, their application is not suitable for ZABs. This might be due to the highly alkaline environment of the ZAB. The addition of biodegradable polymers to the CMC matrix may be an adequate approach to increase the membrane mechanical properties. However, the high KOH concentration prevents the formation of a film. We have therefore fabricated the composite membranes in water, following by KOH adsorption step. These membranes (CMC: biopolymer (1:2) *ex-situ*) presented good self-healing properties as well as large KOH uptake capacity and a low weight loss was observed, being very important for the life of the battery ensuring a non-evaporation of the liquid electrolyte, thus an ad-hoc performance of the battery. In addition, they presented good mechanical stability because they do not liquify. EIS analysis shows remarkably high ionic conductivity of the membranes, especially for CMC:PAA (0.231 Scm^{-1}). The calculated activation energies give a clue of the easiness that have OH- ions to move into the membranes, especially in the CMC:PAA, being just 6.38 kJmol^{-1}, lower than recent references in the literature. Electrochemistry results showed high Zn utilization (78%) for CMC:PAA during galvanostatic discharge at high current density (5 mAcm^{-2}). Furthermore, large gravimetric energy densities were achieved (294.21 Whkg^{-1} for CMC:PVA and 443.19 Whkg^{-1} for CMC:PAA *ex-situ* mem-

Batteries & Supercaps

Research Article
doi.org/10.1002/batt.202200570

Chemistry Europe
European Chemical
Societies Publishing

branes). The membrane CMC:PAA (1:2) *ex-situ* seems the best of the materials developed here, and could be a candidate for further optimization and scale-up as electrolyte for primary ZABs.

Experimental Section

Materials: For gel electrolytes preparation, CMC powder (Carboxymethylcellulose sodium salt, low viscosity, Sigma-Aldrich, Germany), PVA powder (poly(vinyl alcohol), 88% hydrolyzed, average M.W. 88000, Acros Organics, Belgium), PAA powder (poly(acrylic acid) partial potassium salt, <1000 μm particle size, Sigma-Aldrich, Germany), potassium hydroxide (KOH, pellets, extra pure grade, Scharlab, Spain), and distilled water (type II analytical grade, <1 μS cm^{-1}, ECOMATIC, Wasserlab, Spain) were used. For full cells, the anode is obtained by mixing commercial zinc powder (Zn >98%, CEGASA Energía, SLU., Spain) and a 45 wt% KOH solution to form a paste (Zn loading approx. 65% by weight). The cathode for primary cells is a mixture of MnO_2, carbon conductive additive, and poly(tetrafluoroethylene) (PTFE) binder, kindly provided by CEGASA, Spain. All chemicals were used as received without further purification.

FTIR measurements: FTIR measurements were carried out running a Vertex 70 Microscope from Bruker (Billerica, MA, United States). All the sample spectra of materials were recorded under argon flow, corrected for the background, and collected in the wavelength range 4000–400 cm^{-1} as average of 64 repeated scans.

TGA and DTA measurements: TG-DTA were carried out running a STA 449 F3 Jupiter instrument (Netzsch, Germany). All the sample thermograms were recorded under argon flow. The experimental conditions are the following: heating of 5 °C/min under argon atmosphere.

KOH % uptake: CMC:biopolymer (1:2) *ex-situ* membranes were punched with a 3 mm diameter punch tool and weighted. After this, membranes were wetted with an 8 M KOH solution and allowed for swelling for 24 h. The materials were carefully dried with laboratory paper to eliminate the supernatant liquid and to measure the weight of the membranes and thus know how much KOH they have absorbed. These measurements were done at room temperature and using a big crystallizer to cover the samples to prevent from contamination.

$$KOH\ (\%)uptake = \frac{m_f - m_i}{m_i} \cdot 100 \tag{1}$$

where m_f, and m_i are the wet mass after the KOH absorption and the dry mass before the KOH being absorbed.

Weight loss: The *ex-situ* membranes were punched with a 3 mm diameter punch tool and weighted and kept for 50 h separately in room temperature and open system. Then, they were weighted again, and the weight loss was calculated using the following equation:

$$Weight\ loss\ (\%) = 100 - \left(\frac{m_f \times 100}{m_i}\right) \tag{2}$$

where m_f, and m_i are the mass after 50 h of storage and the initial mass weight.

Ionic conductivity measurements: The ionic conductivity was measured by electrochemical impedance spectroscopy (EIS), using a Solartron 1260 A Impedance/Gain-Phase Analyzer (Ametek Inc., Berwyn, PA, United States). The materials were tested in a frequency range from 10 MHz to 100 Hz applying 50 mV as polarization amplitude. The membranes were punched with a 3 mm diameter punch tool and assembled inside a coin cell (type CR2032) with a Teflon sheet punched also with a 3 mm punch tool. The average of, at least, three replicated measures is reported. The value for the electrolyte resistance is obtained from the intercept of the Nyquist plot with the X axis. The ionic conductivity (σ) of the membrane is then calculated using the following equation:

$$\sigma = \frac{t}{A} \cdot \frac{1}{R} \tag{3}$$

where t, A, and R are the thickness, area, and resistance of the membrane, respectively. The thickness of the membrane was measured after performing the EIS measurements. For ionic conductivity measurements as function of temperature, a temperature-controlled incubator (KB-23, Binder Inc., Bohemia, NY, United States) was used.

Cell assembly and electrochemical measurements: Full cells were assembled using an in-house design, consisting of a circular Teflon body with compartments for components. The anode paste is pressed in a circular cavity of 13 mm. on top of it, a membrane disk of 24 mm in diameter is placed, and then approx. 250 mg of cathode covers it, forming approx. a 22 mm diameter cathode area. The assembly is completed by Ni-based current collectors as electrical contacts. A Teflon cap, with two aeration holes, closes the cell. Sealing is ensured by pression thanks to an O-ring and two bolts. The anode area (1.33 cm^2) is used to calculate current densities in all experiments; Zn extractions, specific capacities, and all the other metrics,[13] are normalized by using the theoretical capacity of Zn (819.73 mAh g^{-1}), and masses indicated for each cell. Galvanostatic experiments were performed on a BCS 815 potentiostat (BioLogic, Seyssinet-Pariset, France) to determine the electrochemical behavior membranes. For these primary cells, the current density applied was 5 mA cm^{-2}, with a cut-off voltage of 0.8 V.

Conflict of Interest

The authors declare no conflict of interest.

Data Availability Statement

Research data are not shared.

Batteries & Supercaps

Research Article
doi.org/10.1002/batt.202200570

Chemistry Europe

European Chemical
Societies Publishing

[1] S. Lorca, F. Santos, A. J. Fernández Romero, *Polymers (Basel).* **2020**, *12*, 2812.

[2] M. T. Tsehaye, F. Alloin, C. Iojoiu, R. A. Tufa, D. Aili, P. Fischer, S. Velizarov, *J. Power Sources* **2020**, *475*, 228689.

[3] Y. Xu, X. Xu, M. Guo, G. Zhang, Y. Wang, *Front. Chem.* **2022**, *10*.

[4] S. Hosseini, S. Masoudi Soltani, Y.-Y. Li, *Chem. Eng. J.* **2021**, *408*, 127241.

[5] P. Zhang, K. Wang, P. Pei, Y. Zuo, M. Wei, X. Liu, Y. Xiao, J. Xiong, *Mater. Today Chem.* **2021**, *21*, 100538.

[6] W. G. Moon, G.-P. Kim, M. Lee, H. D. Song, J. Yi, *ACS Appl. Mater. Interfaces* **2015**, *7*, 3503.

[7] C. Y. Chan, Z. Wang, H. Jia, P. F. Ng, L. Chow, B. Fei, *J. Mater. Chem. A* **2021**, *9*, 2043.

[8] H. Dong, J. Li, J. Guo, F. Lai, F. Zhao, Y. Jiao, D. J. L. Brett, T. Liu, G. He, I. P. Parkin, *Adv. Mater.* **2021**, *33*, 2007548.

[9] R. Gilliam, J. Graydon, D. Kirk, S. Thorpe, *Int. J. Hydrogen Energy* **2007**, *32*, 359.

[10] E. Lizundia, D. Kundu, *Adv. Funct. Mater.* **2021**, *31*, 2005646.

[11] D. E. Ciolacu, D. M. Suflet, In *Biomass as Renewable Raw Material to Obtain Bioproducts of High-Tech Value*, Elsevier, **2018**, pp. 401–439.

[12] M. Klein, E. Poverenov, *J. Sci. Food Agric.* **2020**, *100*, 2337.

[13] D. Frattini, E. García-Gaitán, A. Bustinza Murguialday, M. Armand, N. Ortiz Vitoriano, *Energy Environ. Sci.* **2022**.

[14] J. Fu, J. Zhang, X. Song, H. Zarrin, X. Tian, J. Qiao, L. Rasen, K. Li, Z. Chen, *Energy Environ. Sci.* **2016**, *9*, 663.

[15] J. Fu, F. M. Hassan, J. Li, D. U. Lee, A. R. Ghannoum, G. Lui, Md. A. Hoque, Z. Chen, *Adv. Mater.* **2016**, *28*, 6421.

[16] X. Zhu, H. Yang, Y. Cao, X. Ai, *Electrochim. Acta* **2004**, *49*, 2533.

[17] O. Kwon, H. J. Hwang, Y. Ji, O. S. Jeon, J. P. Kim, C. Lee, Y. G. Shul, *Sci. Rep.* **2019**, *9*, 3175.

[18] G. M. Wu, S. J. Lin, C. C. Yang, *J. Membr. Sci.* **2006**, *280*, 802.

[19] S. Nasibi, H. Nargesi khoramabadi, M. Arefian, M. Hojjati, I. Tajzad, A. Mokhtarzade, M. Mazhar, A. Jamavari, *J. Comp. Compd.* **2020**, *2*, 68.

[20] C. Tang, B. Wang, H. Wang, Q. Zhang, *Adv. Mater.* **2017**, *29*, 1703185.

[21] X. Fan, J. Liu, J. Ding, Y. Deng, X. Han, W. Hu, C. Zhong, *Front. Chem.* **2019**, *7*.

[22] S. Peng, X. Han, L. Li, S. Chou, D. Ji, H. Huang, Y. Du, J. Liu, S. Ramakrishna, *Adv. Energy Mater.* **2018**, *8*, 1800612.

[23] Y. Guo, P. Yuan, J. Zhang, Y. Hu, I. S. Amiinu, X. Wang, J. Zhou, H. Xia, Z. Song, Q. Xu, S. Mu, *ACS Nano* **2018**, *12*, 1894.

[24] Y. Li, C. Zhong, J. Liu, X. Zeng, S. Qu, X. Han, Y. Deng, W. Hu, J. Lu, *Adv. Mater.* **2018**, *30*, 1703657.

[25] Z. Song, X. Liu, J. Ding, J. Liu, X. Han, Y. Deng, C. Zhong, W. Hu, *ACS Appl. Mater. Interfaces* **2022**.

[26] D. Wu, P. R. Chang, X. Ma, *Carbohydr. Polym.* **2011**, *86*, 877.

[27] F. Santos, J. P. Tafur, J. Abad, A. J. Fernández Romero, *J. Electroanal. Chem.* **2019**, *850*, 113380.

[28] H. S. Mansur, C. M. Sadahira, A. N. Souza, A. A. P. Mansur, *Mater. Sci. Eng. C* **2008**, *28*, 539.

[29] B. Kumar, F. Deeba, R. Priyadarshi, Sauraj, S. Bano, A. Kumar, Y. S. Negi, *Polym. Bull.* **2020**, *77*, 4555.

[30] M. A. Moharram, M. A. Allam, *J. Appl. Polym. Sci.* **2007**, *105*, 3220.

[31] E. J. Price, J. Covello, A. Tuchler, G. E. Wnek, *ACS Appl. Mater. Interfaces* **2020**, *12*, 18997.

[32] M. F. Bósquez-Cáceres, L. de Lima, V. Morera Córdova, A. D. Delgado, J. Béjar, N. Arjona, L. Álvarez-Contreras, J. P. Tafur, *Batteries* **2022**, *8*, 265.

[33] A. Lewandowski, K. Skorupska, J. Malinska, *Solid State Ionics* **2000**, *133*, 265.

[34] Q. Liu, R. Liu, C. He, C. Xia, W. Guo, Z.-L. Xu, B. Y. Xia, *eScience* **2022**, *2*, 453.

[35] T. Fekete, J. Borsa, E. Takács, L. Wojnárovits, *Rad. Phys. Chem.* **2016**, *124*, 135.

[36] E. R. Ezeigwe, L. Dong, R. Manjunatha, M. Tan, W. Yan, J. Zhang, *Nano Energy* **2021**, *84*, 105907.

[37] S. Zhao, D. Xia, M. Li, D. Cheng, K. Wang, Y. S. Meng, Z. Chen, J. Bae, *ACS Appl. Mater. Interfaces* **2021**, *13*, 12033.

[38] K. Lu, T. Jiang, H. Hu, M. Wu, *Front. Chem.* **2020**, *8*.

[39] J. Li, L. Geng, G. Wang, H. Chu, H. Wei, *Chem. Mater.* **2017**, *29*, 8932.

[40] M. N. Hafiza, M. I. N. Isa, *Iop. Conf. Ser. Mater. Sci. Eng.* **2018**, *440*, 012039.

[41] Y. Lu, T. Zhu, N. Xu, K. Huang, *ACS Appl. Energ. Mater.* **2019**, *2*, 6904.

[42] A. Mohamad, N. S. Mohamed, M. Z. A. Yahya, R. Othman, S. Ramesh, Y. Alias, A. K. Arof, *Solid State Ionics* **2003**, *156*, 171.

[43] C.-C. Yang, S.-J. Lin, *J. Power Sources* **2002**, *112*, 497.

[44] C.-C. Yang, *Mater. Lett.* **2004**, *58*, 33.

[45] S. Zhao, T. Liu, Y. Dai, Y. Wang, Z. Guo, S. Zhai, J. Yu, C. Zhi, M. Ni, *Chem. Eng. J.* **2022**, *430*, 132718.

[46] Q. Wang, Q. Feng, Y. Lei, S. Tang, L. Xu, Y. Xiong, G. Fang, Y. Wang, P. Yang, J. Liu, W. Liu, X. Xiong, *Nat. Commun.* **2022**, *13*, 3689.

[47] S. Qu, Z. Song, J. Liu, Y. Li, Y. Kou, C. Ma, X. Han, Y. Deng, N. Zhao, W. Hu, C. Zhong, *Nano Energy* **2017**, *39*, 101.

[48] H. Arai, M. Hayashi, In *Encyclopedia of Electrochemical Power Sources*, Elsevier, **2009**, pp. 55–61.